Knockdown of lncRNA ANRIL suppresses the production of inflammatory cytokines and mucin 5AC in nasal epithelial cells via the miR-15a-5p/JAK2 axis

HUO-WANG LIU[1,2], ZHONG-LIANG HU[3], HAO LI[2], QI-FENG TAN[2], JING TONG[2] and YONG-QUAN ZHANG[1]

[1]Department of Otolaryngology-Head and Neck Surgery, The Third Xiangya Hospital, Central South University, Changsha, Hunan 410013; [2]Department of Otolaryngology-Head and Neck Surgery, The Fifth Affiliated Hospital of Xinjiang Medical University, Urumqi, Xinjiang 830000; [3]Department of Pathology, Xiangya Hospital, Central South University, Changsha, Hunan 410007, P.R. China

Abstract. The incidence of allergic rhinitis (AR) is increasing worldwide. Human nasal epithelial cells (HNECs) are the key cells in the occurrence of AR. Antisense non-coding RNA in the INK4 locus (ANRIL) was discovered to be involved in the progression of AR. However, the mechanism by which ANRIL mediates the progression of AR remains to be determined. The present study aimed to further explore the mechanism by which ANRIL regulates AR. Thereby, HNECs were treated with IL-13 to mimic AR *in vitro*. The mRNA expression levels of ANRIL, microRNA (miR)-15a-5p, JAK2, mucin 5AC (MUC5AC), granulocyte-macrophage colony-stimulating factor (GM-CSF) and eotaxin-1, and protein expression levels of JAK2, STAT3 and phosphorylated-STAT3 in HNECs were analyzed using reverse transcription-quantitative PCR and western blotting, respectively. ELISAs were used to detect the secretory levels of inflammatory cytokines and mucin in cell supernatants. In addition, a dual luciferase reporter assay was used to confirm the downstream target of ANRIL and the target gene of miR-15a-5p. The results revealed that the secretory levels of eotaxin-1, GM-CSF and MUC5AC were significantly upregulated by IL-13 in the supernatant of HNECs. The expression levels of ANRIL and JAK2 were also upregulated in IL-13-induced HNECs, while the expression levels of miR-15a-5p were downregulated. In addition, ANRIL was identified to bind to miR-15a-5p. The IL-13-induced upregulation of eotaxin-1, GM-CSF and MUC5AC mRNA expression and secretory levels was significantly inhibited by the genetic knockdown of ANRIL, while the miR-15a-5p inhibitor effectively reversed this effect. JAK2 was also discovered to be directly targeted by miR-15a-5p. The overexpression of JAK2 significantly suppressed the therapeutic effect of miR-15a-5p mimics on IL-13-induced inflammation *in vitro*. In conclusion, the findings of the present study suggested that the genetic knockdown of ANRIL may suppress the production of inflammatory cytokines and mucin in IL-13-treated HNECs via regulation of the miR-15a-5p/JAK2 axis. Thus, ANRIL may serve as a novel target for AR treatment.

Introduction

The incidence of allergic rhinitis (AR) has been increasing over the past decades in Asian countries (1). In China, the frequency of AR has increased from 11 to 17% in the past 10 years (2). AR is an immune-related disease that is characterized as an IgE-modulated type I hypersensitivity disorder (3). However, type 2 helper T (Th2) cells have also been proposed to mediate nasal allergic diseases (4). In addition, IL-13, which is a cytokine produced by Th2 cells, was verified to a key regulator of the pathogenesis caused by immune-related inflammation (5). IL-13 can activate eosinophils and promote the production of mucus and growth factors via the regulation of epithelial cells (6). IL-13-treated human nasal epithelial cells (HNECs) are frequently used as an in vitro model for the study of AR (7). Thus, the modulation of IL-13 is of great significance for the treatment of AR.

Long non-coding RNAs (lncRNAs) are transcripts of ~200-10,0000 nucleotides in length that are not translated into proteins (8,9). lncRNAs have been confirmed to serve important biological roles in numerous biological processes, including DNA damage, programmed cell death and inflammation (10-12). Furthermore, lncRNAs have also been reported to participate in the pathogenesis of AR (13-15). For example,

Correspondence to: Dr Yong-Quan Zhang, Department of Otolaryngology-Head and Neck Surgery, The Third Xiangya Hospital, Central South University, 138 Tongzipo Road, Yuelu, Changsha, Hunan 410013, P.R. China
E-mail: zyq2321@126.com

antisense non-coding RNA in the INK4 locus (ANRIL) was found to be associated with an increased AR risk and severity, in addition to an enhanced inflammatory status (16). However, the mechanism by which ANRIL mediates the progression of AR remains to be determined.

MicroRNAs (miRNAs/miRs) are a class of non-coding small RNAs that bind to the 3'-untranslated region (3'-UTR) of mRNA to regulate mRNA expression (17-19). miRNAs have been proven to be involved in various cellular processes, including cell growth, differentiation and metabolic progression (20-24). The dysregulation of miRNAs has also been confirmed in AR, suggesting the potential function of miRNAs in AR (25,26). For instance, miR-498 was discovered to be activated in tissues from patients with AR, and the suppression of miR-498 promoted inflammatory responses caused by IL-13 and mucin production in HNECs (15). Moreover, the expression levels of miR-487b were reported to be upregulated in patients with AR, which mitigated the pathological alterations of AR by inhibiting the expression levels of IL-33 and homolog of sulfotransferase (27). In addition, miR-15a-5p expression levels were reportedly downregulated in patients with AR, where served an inhibitory effect in AR (28). However, the association between ANRIL and miR-15a-5p in AR remains unclear.

JAK2/STAT3 signaling was found to function as a crucial mediator in the overactivation of macrophages, which caused an increase in proinflammatory cytokine production (29). In addition, it was reported that miR-375 alleviated the progression of AR via regulation of the JAK2/STAT3 axis (30). Based on these findings, it was hypothesized that JAK2/STAT3 signaling may serve an important role in the progression of AR.

The present study aimed to confirm the role of ANRIL in AR. In addition, the study aimed to further determine the mechanism by which ANRIL mediated the progression of AR. The results of the current study may provide a novel strategy for the treatment of AR.

Materials and methods

Cell culture and treatment. Primary HNECs (cat. no. HUM-iCell-m018) and 293T cell lines (cat. no. ACS-4500) were purchased from iCell Bioscience, Inc., and the American Type Culture Collection, respectively. All cells were cultured in RPMI-1640 medium (Gibco; Thermo Fisher Scientific, Inc.) supplemented with 10% FBS (Gibco; Thermo Fischer Scientific, Inc.), 1% penicillin (Invitrogen; Thermo Fisher Scientific, Inc.) and 1% streptomycin (Invitrogen; Thermo Fischer Scientific, Inc.), and maintained at 37°C and 5% CO_2. To establish an *in vitro* model of AR, HNECs were treated with 50 ng/ml IL-13 (Sigma-Aldrich; Merck KGaA) at 37°C for 24 h, as previously described (31). The control group consisted of untreated cells.

Cell transfection. Cell transfection was performed according to a previously reported experimental method (32). The miR-15a-5p inhibitor, miR-15a-5p mimic and their respective negative controls (NCs) were purchased from Shanghai GenePharma Co., Ltd. The sequences were as follows: miR-15a-5p mimics sense, 5'-UAGCAGCACAUAAUGGUUUGUG-3' and antisense, 5'-CAAACCAUUAUGUGCUGCUAUU-3'; mimic

NC sense, 5'-UUCUCCGAACGUGUCACGUTT-3' and antisense, 5'-ACGUGACACGUUCGGAGAATT-3'; miR-15a-5p inhibitor, 5'-CACAAACCAUUAUGUGCUGCUA-3'; and inhibitor NC, 5'- CAGUACUUUUGUGUAGUACAA-3'. For the genetic knockdown of ANRIL, the corresponding short hairpin RNA (shRNA/sh) targeting ANRIL (sh-ANRIL) and the non-targeting control shRNA (sh-NC) were cloned into the pSicoR vector (Addgene, Inc.). pcDNA3.1-JAK2 and the corresponding control (empty pcDNA3.1 vector) were obtained from GenScript. HNECs ($5x10^3$ per well) were transfected using Lipofectamine® 2000 reagent (Invitrogen; Thermo Fisher Scientific, Inc.). Briefly, the cells were cultured in antibiotic-free medium (RPMI-1640) at 37°C for 24 h, and transfections were performed upon the cell confluence reaching 90%. The successfully constructed vectors, miR-15a-5p inhibitor/mimics or controls, and Lipofectamine 2000 were diluted (1:100) in serum-free Opti-MEM medium (Gibco; Thermo Fisher Scientific, Inc.), mixed after standing for 5 min, and then incubated for 20 min at room temperature. Then, 100 μl of the mixed solution was added to the cells in each well and incubated at 37°C for 48 h. The medium was replaced with fresh medium after 6 h. Reverse transcription-quantitative PCR (RT-qPCR) was used to confirm the transfection efficiency 48 h after transfection.

RT-qPCR. RT-qPCR analysis was used to analyze mRNA expression levels, as previously described (33). Briefly, total RNA was extracted from HNECs using TRIzol® reagent (Invitrogen; Thermo Fisher Scientific, Inc.), according to the manufacturer's protocol. The quality and quantity of RNA was detected using 10% agarose gel electrophoresis. In addition, A260/A280 ratios were calculated using a spectrophotometer (NanoDrop Technologies; Thermo Fisher Scientific, Inc.), and a ratio between 1.8 and 2.0 indicated that the extracted RNA was qualified. Total RNA was reverse transcribed into cDNA using the PrimeScript RT reagent kit (Takara Bio, Inc.), according to the manufacturer's protocol. qPCR was subsequently performed using the SYBR Premix Ex Taq II kit (Takara Bio, Inc.). The following thermocycling conditions were used for the qPCR: Initial denaturation for 1 min at 95°C; followed by 35 cycles for 15 sec at 95°C and 30 sec at 60°C. The primer pairs used are presented in Table I. The expression levels were quantified using the $2^{-\Delta\Delta Cq}$ method (34). GAPDH or U6 were used as the internal loading control for quantification. Each experiment was performed in triplicate.

Western blotting. Protein expression levels were analyzed using western blotting, according to a previous study (35). Briefly, total protein was extracted from HNECs using RIPA lysis buffer [50 mM Tris (pH 7.4), 150 mM NaCl, 1% Triton X-100, 1% sodium deoxycholate, 0.1% SDS, 2 mM sodium pyrophosphate, 25 mM β-glycerophosphate, 1 mM EDTA, 1 mM Na_3VO_4 and 0.5 μg/ml leupeptin] (Beyotime Institute of Biotechnology). Total protein was quantified using a bicinchoninic acid protein kit (Pierce; Thermo Fisher Scientific, Inc.) on a Multiskan™ FC microplate photometer (562 nm; Thermo Fisher Scientific, Inc.) and 40 μg protein/lane was separated via 10% SDS-PAGE. The separated proteins were subsequently transferred onto PVDF membranes (Invitrogen; Thermo Fisher Scientific, Inc.) and blocked with

Table I. Primer sequences used for reverse transcription-quantitative PCR.

Gene	Primer sequence (5'→3')
Antisense non-coding RNA in the INK4 locus	F: GCCGGACTAGTGTCCCTTTT
	R: TCGGGAAAGGATTCCAGCAC
MicroRNA-15a-5p	F: CGGCTAGCAGCACATAATGG
	R: GTCGTATCCAGTGCAGGGTCCGAGG TATTCGCACTGGATACGACCACAAA
JAK2	F: CCAAAGTGGGCAGAATTAGC
	R: GTGTAGGATCCCGGTCTTCA
Granulocyte-macrophage colony-stimulating factor	F: GAGAGCTCCCAGCCTAAGGT
	R: TGCACACCTCTTGACACTCC
Eotaxin-1	F: CGGATACCTTGGCGCTAGTA
	R: TCACTCCGTCTTTTGCACAG
Mucin 5AC	F: AGCCCAAGATGCCCTTCAGT
	R: CCGTGTTCCTACCCCCAATG
U6	F: GGTCGGGCAGGAAAGAGGGC
	R: GCTAATCTTCTCTGTATCGTTCC
GAPDH	F: CTGACTTCAACAGCGACACC
	R: GTGGTCCAGGGGTCTTACTC

F, forward; R, reverse.

5% skimmed milk in TBS with 10% Tween 20 for 1 h at room temperature. The membranes were then incubated with the following primary antibodies overnight at 4˚C (all from Abcam): Anti-JAK2 (1:1,000; cat. no. ab108596), anti-STAT3 (1:2,000; cat. no. ab68153), anti-phosphorylated (p)-STAT3 (1:2,000; cat. no. ab76315) and anti-GAPDH (1:1,000; cat. no. ab9485). Following the primary antibody incubation, the PVDF membranes were washed with TBS with Tween-20 and incubated with a HRP-conjugated secondary antibody (1:5,000; cat. no. ab205718; Abcam) at room temperature for 1 h. Finally, the protein bands were visualized using an ECL detection kit (Beyotime Institute of Biotechnology). The relative protein expression levels were normalized to GAPDH expression levels. Image-Pro Plus 6.0 (National Institutes of Health) was used for the densitometry analysis.

Dual luciferase reporter assay. miR-15a-5p binding sites were identified by StarBase database (http://starbase.sysu.edu.cn). The dual luciferase reporter assay was performed according to a previous study (36). ANRIL and JAK2 3'-UTRs containing the putative binding sites (GCUGCU) of miR-15a-5p were synthetized and obtained from Sangon Biotech Co., Ltd. The aforementioned sequences were cloned into the pmirGLO vector (Promega Corporation) to construct wild-type (WT) or mutant (MUT) ANRIL (10 nM) and JAK2 reporter vectors (10 nM). Point mutations of the miR-15a-5p binding sites were generated using a Site-Directed Mutagenesis kit (Promega Corporation). The WT or MUT ANRIL/JAK2 vectors (10 nM) were co-transfected into HNECs ($5x10^6$ per well) with mimics NC or miR-15a-5p mimics (10 nM) using Lipofectamine 2000 reagent for 24 h at 37˚C, according to the manufacturer's instructions. After 24 h, relative luciferase

activities were detected using a Dual-GLO Luciferase assay system (Promega Corporation). Firefly luciferase activity was normalized to *Renilla* luciferase activity.

ELISA. The secretory levels of eotaxin-1 [cat. no. 70-EK1130-96; Hangzhou Multi Sciences (Lianke) Biotech Co., Ltd.), granulocyte-macrophage colony-stimulating factor [(GM-CSF); cat. no. 70-EK163HS-96; Hangzhou Multi Sciences (Lianke) Biotech Co., Ltd.] and mucin 5AC [(MUC5AC); cat. no. ml-1016017; Shanghai Enzyme-linked Biotechnology Co., Ltd.] in the supernatant of HNECs were analyzed using ELISA kits. The supernatants of HNECs were harvested by centrifugation (100 x g, 20 min, 4˚C). Subsequently, the cells were incubated with a HRP-conjugated secondary antibody, which was included in the ELISA kits, at room temperature for 1 h. Finally, after incubation with hydrochloric acid (100 μl) at room temperature until the solution became discolored, the absorbance was measured using a microplate reader (450 nm).

Statistical analysis. Statistical analysis was performed using SPSS 22.0 software (IBM Corp.). Data are presented as the mean ± SD and three technical repeats were performed in three biological replicate experiments. Statistical differences between 2 groups were analyzed using an unpaired Student's t-test, while ≥3 groups were analyzed using a one-way ANOVA followed by a Tukey's post hoc test. $P<0.05$ was considered to indicate a statistically significant difference.

Results

ANRIL and JAK2 expression levels are upregulated in IL-13-induced HNECs, while miR-15a-5p expression levels are
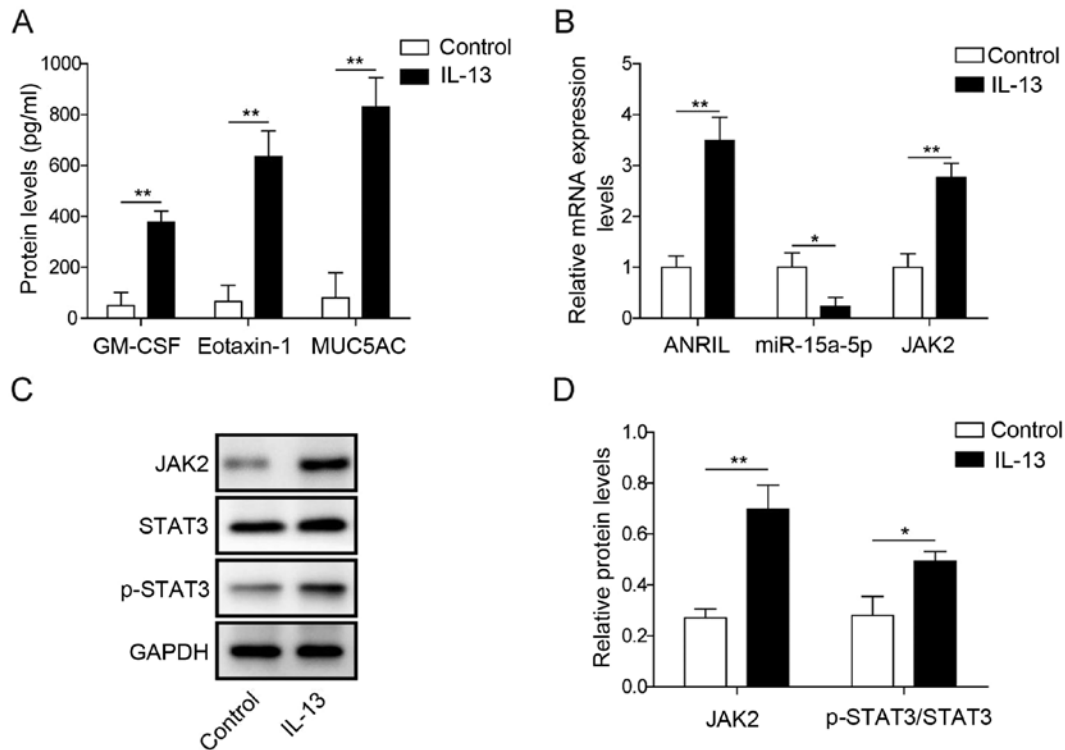
Figure 1. ANRIL and JAK2 expression levels are upregulated in IL-13-induced HNECs, while miR-15a-5p expression levels are downregulated. HNECs were treated with 50 ng/ml IL-13 for 24 h. (A) Secretory levels of eotaxin-1, GM-CSF and MUC5AC in HNEC supernatants were analyzed using ELISAs. (B) Relative mRNA expression levels of ANRIL, miR-15a-5p and JAK2 in HNECs were analyzed using reverse transcription-quantitative PCR. (C) Protein expression levels of JAK2, STAT3 and p-STAT3 in HNECs were analyzed using western blotting. (D) Relative protein expression levels from part (C) were semi-quantified via normalization to GAPDH expression levels. *$P<0.05$, **$P<0.01$. ANRIL, antisense non-coding RNA in the INK4 locus; HNECS, human nasal epithelial cells; GM-CSF, granulocyte-macrophage colony-stimulating factor; MUC5AC, mucin 5AC; miR, microRNA; p-, phosphorylated.

downregulated. To establish an *in vitro* model of AR, HNECs were treated with IL-13 for 24 h. As indicated in Fig. 1A, the secretory levels of eotaxin-1, GM-CSF and MUC5AC in HENC supernatants were significantly upregulated by IL-13 stimulation. These data suggested that an *in vitro* model of AR was successfully established. In addition, the mRNA expression levels of ANRIL and JAK2 in HNECs were significantly upregulated in the presence of IL-13 compared with the control group (Fig. 1B). In contrast, miR-15a-5p expression levels in HNECs were significantly downregulated following IL-13 stimulation compared with the control group (Fig. 1B). Furthermore, the protein expression levels of JAK2 and p-STAT3/STAT3 in HNECs were significantly upregulated by IL-13 stimulation compared with the control group (Fig. 1C and D). These data indicated that ANRIL and JAK2 may promote the occurrence of AR, while miR-15a-5p exhibited the opposite effects.

ANRIL sponges miR-15a-5p in HNECs. To confirm the transfection efficiency of sh-ANRIL in HNECs, RT-qPCR analysis was performed. As shown in Fig. 2A, the expression levels of ANRIL in HNECs were significantly downregulated following transfection with sh-ANRIL. These results confirmed that sh-ANRIL was stably transfected into HNECs. The genetic silencing of ANRIL significantly upregulated the expression levels of miR-15a-5p in HNECs (Fig. 2B). These data suggested that ANRIL may negatively regulate miR-15a-5p expression levels. The expression levels of miR-15a-5p

in HNECs were significantly upregulated following the transfection with the miR-15a-5p mimics and downregulated in the presence of the miR-15a-5p inhibitor compared with their respective NC groups (Fig. 2C). Furthermore, to identify the downstream target gene of ANRIL, the StarBase database and dual luciferase reporter assays were used. The StarBase database predicted that ANRIL bound to miR-15a-5p (Fig. 2D). Subsequent dual luciferase reporter assays revealed that the co-transfection with miR-15a-5p mimics significantly suppressed the relative luciferase activity of ANRIL-WT compared with cells co-transfected with the ANRIL-WT vector and mimics NC, while no significant differences were observed in the relative luciferase activity of ANRIL-MUT between the cells co-transfected with the mimics NC or miR-15a-5p mimics (Fig. 2D). These findings suggested that ANRIL may bind to miR-15a-5p in HNECs.

ANRIL regulates the production of inflammatory cytokines and mucin via inhibition of miR-15a-5p. Since eotaxin-1, GM-CSF and MUC5AC have been discovered to serve promoting roles in AR (15,37), the effect of ANRIL on these cytokines and mucin was investigated. As shown in Fig. 3A-C, the mRNA expression levels of GM-CSF, eotaxin-1 and MUC5AC in HNECs were significantly upregulated by IL-13 stimulation; however, the expression levels of the aforementioned genes were significantly reversed in the presence of sh-ANRIL. Conversely, co-transfection with the miR-15a-5p inhibitor partially reversed the effect of ANRIL knockdown
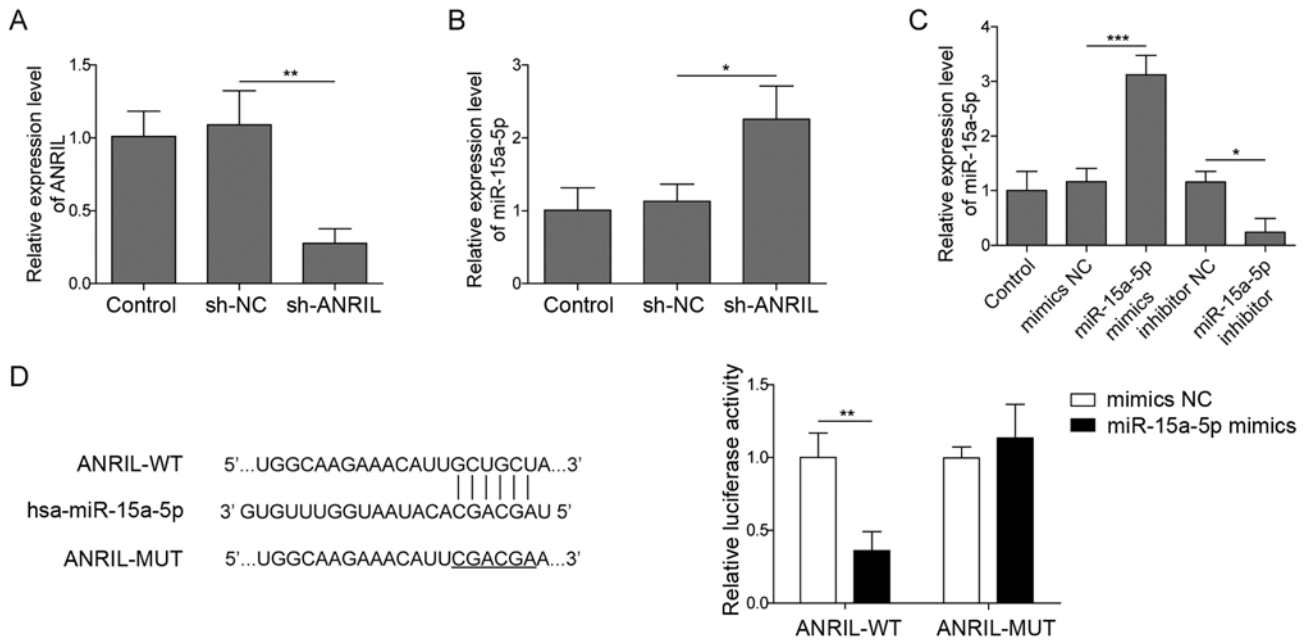
Figure 2. ANRIL binds to miR-15a-5p in HNECs. HNECs were transfected with sh-ANRIL or sh-NC for 24 h. (A) Transfection efficiency was confirmed using RT-qPCR. (B) miR-15a-5p expression levels in HNECs were analyzed using RT-qPCR. (C) HNECs were transfected with mimics/inhibitor NC or miR-15a-5p mimics/inhibitor for 24 h. Then, the transfection efficiency was determined using RT-qPCR. (D) Complementary binding between ANRIL and miR-15a-5p was predicted by StarBase. The relative luciferase activity was analyzed following the co-transfection with mimics NC or miR-15a-5p mimics and luciferase reporter plasmids carrying the ANRIL-WT or MUT 3'-untranslated region in HNECs using a dual luciferase reporter assay. $^*P<0.05$, $^{**}P<0.01$, $^{***}P<0.001$. ANRIL, antisense non-coding RNA in the INK4 locus; HNECS, human nasal epithelial cells; sh, short hairpin RNA; NC, negative control; RT-qPCR, reverse transcription-quantitative PCR; miR, microRNA; WT, wild-type; MUT, mutant.
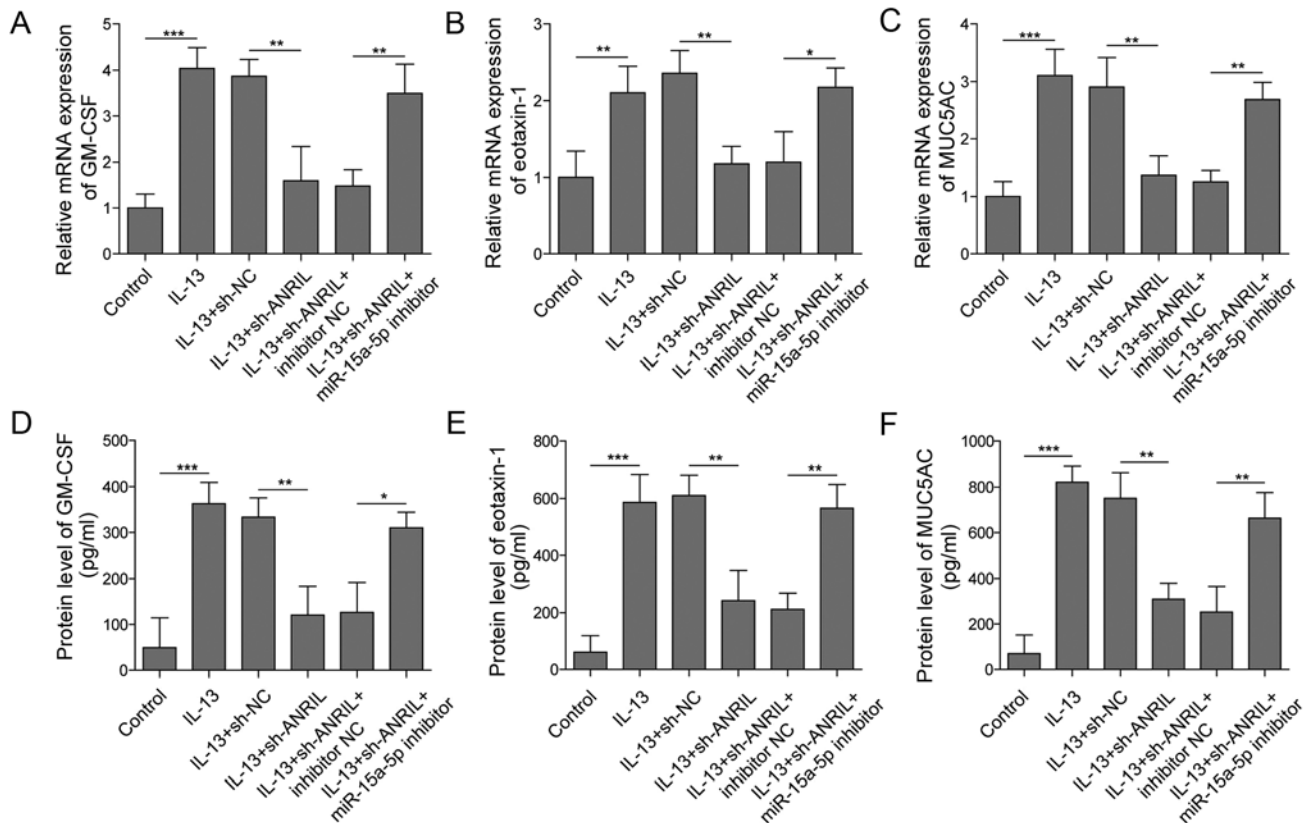

Figure 3. ANRIL regulates the production of inflammatory cytokines and mucin by sponging miR-15a-5p. HNECs were treated with IL-13, IL-13 + sh-NC, IL-13 + sh-ANRIL, IL-13 + sh-ANRIL+ inhibitor NC or IL-13 + sh-ANRIL + miR-15a-5p inhibitor. mRNA expression levels of (A) GM-CSF, (B) eotaxin-1 and (C) MUC5AC in HNECs were analyzed using reverse transcription-quantitative PCR. Secretory levels of (D) GM-CSF, (E) eotaxin-1 and (F) MUC5AC in the supernatants of HNECs were detected using ELISAs. $^*P<0.05$, $^{**}P<0.01$, $^{***}P<0.001$. ANRIL, antisense non-coding RNA in the INK4 locus; HNECS, human nasal epithelial cells; miR, microRNA; sh, short hairpin RNA; NC, negative control; GM-CSF, granulocyte-macrophage colony-stimulating factor; MUC5AC, mucin 5AC.
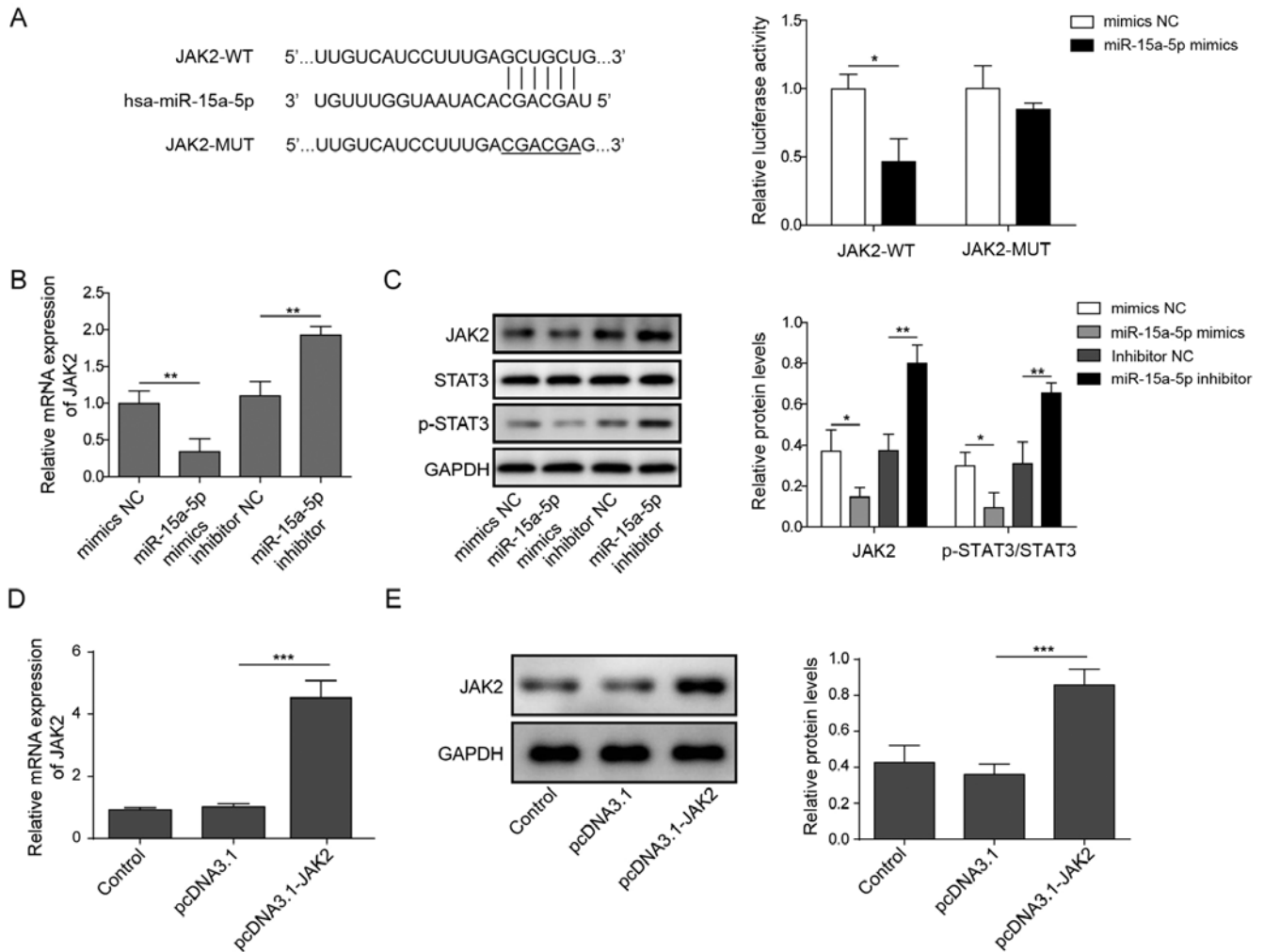
Figure 4. miR-15a-5p inactivates JAK2/STAT3 signaling by directly targeting JAK2. (A) Interaction between JAK2 and miR-15a-5p was predicted using StarBase. The relative luciferase activity was analyzed following the co-transfection with mimics NC/miR-15a-5p mimics and luciferase reporter plasmids carrying JAK2-WT or MUT 3'-untranslated regions. (B) Expression levels of JAK2 in HNECs were analyzed using RT-qPCR. (C) Protein expression levels of JAK2, STAT3 and p-STAT3 in HNECs were analyzed using western blotting. (D) Relative mRNA expression levels of JAK2 in HNECs transfected with pcDNA3.1-JAK2 were analyzed using RT-qPCR. (E) Relative protein expression levels of JAK2 were analyzed using western blotting. The relative protein expression levels were semi-quantified by normalization to GAPDH expression. $^*P<0.05$, $^{**}P<0.01$, $^{***}P<0.001$. miR, microRNA; NC, negative control; WT, wild-type; MUT, mutant; p-, phosphorylated; HNECs, human nasal epithelial cells.

on the mRNA expression levels of these cytokines and mucin. Similar results were obtained regarding the secretory levels of eotaxin-1, GM-CSF and MUC5AC using ELISAs; the IL-13-induced increase in eotaxin-1, GM-CSF and MUC5AC concentrations in HNECs were significantly inhibited by silencing ANRIL, while the inhibitory effect of ANRIL silencing was partially rescued following the co-transfection with the miR-15a-5p inhibitor (Fig. 3D-F). Altogether, these results suggested that the miR-15a-5p inhibitor may significantly reduce the anti-inflammatory effect of ANRIL knockdown on IL-13-induced AR *in vitro*.

miR-15a-5p inactivates JAK2/STAT3 signaling by directly targeting JAK2. To determine the direct target of miR-15a-5p, the StarBase database and dual luciferase reporter assays were used. The analysis indicated that JAK2 might be a direct target of miR-15a-5p (Fig. 4A). Furthermore, the co-transfection with the miR-15a-5p mimics significantly decreased the relative luciferase activity of the JAK2-WT

vector compared with the co-transfection with the mimics NC, but no significant differences were observed in the relative luciferase activity of the JAK2-MUT between the mimics NC and miR-15a-5p mimics group (Fig. 4A). Moreover, the expression levels of JAK2 in HNECs were significantly downregulated following the transfection with the miR-15a-5p mimics compared with the mimics NC group (Fig. 4B). In contrast, the miR-15a-5p inhibitor exhibited the opposite effect (Fig. 4B). The protein expression levels of JAK2 and p-STAT3/STAT3 in HNECs were also significantly downregulated in the miR-15a-5p mimics group compared with the mimics NC group, while the expression levels were significantly upregulated by the miR-15a-5p inhibitor compared with the inhibitor NC (Fig. 4C). Meanwhile, to investigate the association between miR-15a-5p and JAK2, HNECs were treated with pcDNA3.1-JAK2 overexpression vector. The data confirmed that the mRNA and protein expression levels of JAK2 were significantly upregulated in HNECs transfected with pcDNA3.1-JAK2 (Fig. 4D and E).
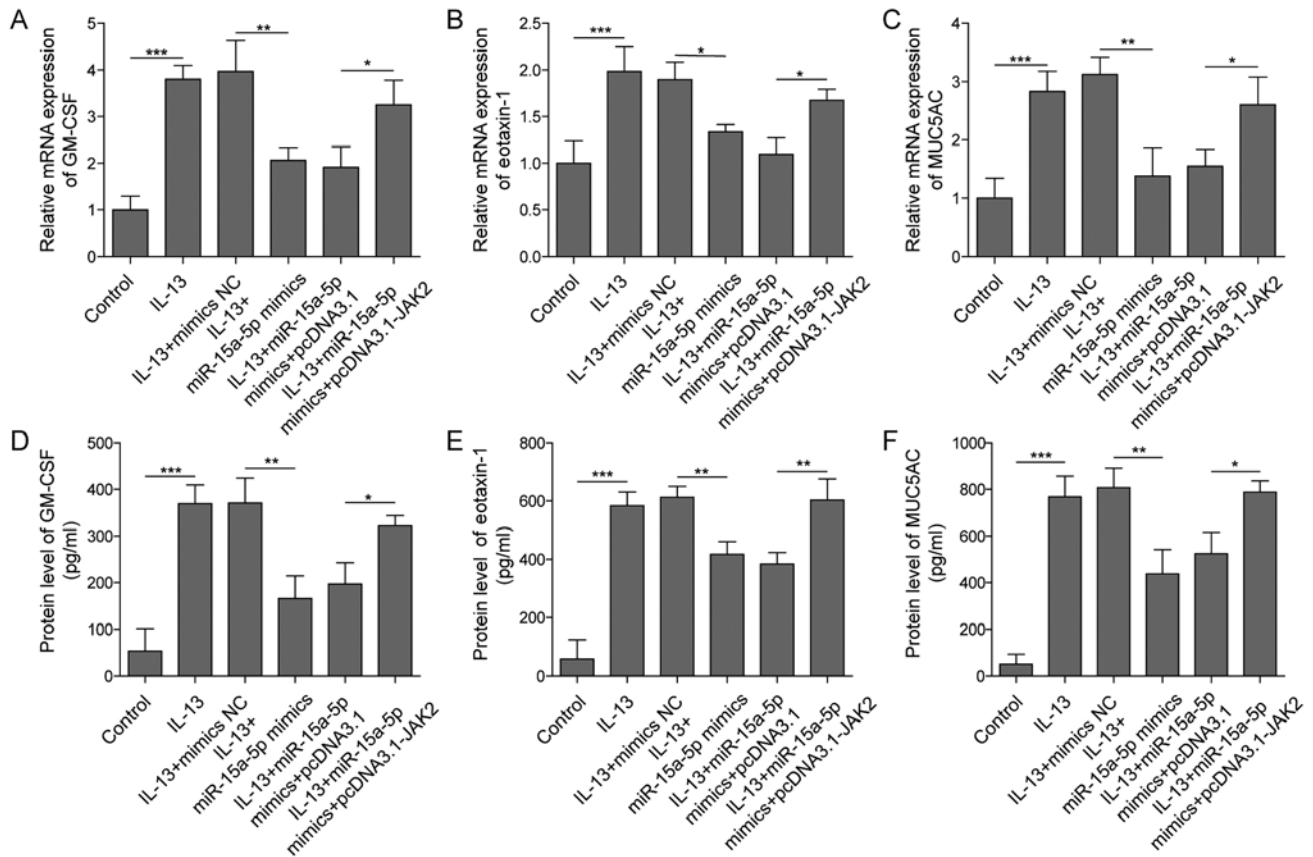
Figure 5. miR-15a-5p mimics significantly reverse the IL-13-induced inflammation in HNECs by targeting JAK2. HNECs were treated with IL-13, IL-13+mimics-NC, IL-13+ miR-15a-5p mimics, IL-13+miR-15a-5p mimics+pcDNA3.1 or IL-13+miR-15a-5p mimics+pcDNA3.1-JAK2. The mRNA expression levels of (A) GM-CSF, (B) eotaxin-1 and (C) MUC5AC in HNECs were analyzed using reverse transcription-quantitative PCR. The secretory levels of (D) GM-CSF, (E) eotaxin-1 and (F) MUC5AC in the supernatants of HNECs were analyzed using ELISA kits. *P<0.05, **P<0.01, ***P<0.001. HNECS, human nasal epithelial cells; miR, microRNA; NC, negative control; GM-CSF, granulocyte-macrophage colony-stimulating factor; MUC5AC, mucin 5AC.

These findings suggested that miR-15a-5p may directly target JAK2 to inhibit the STAT3 signaling pathway.

miR-15a-5p mimics significantly reverse IL-13-induced inflammatory responses in HNECs by targeting JAK2. To further confirm the mechanism by which miR-15a-5p mediated the development of AR *in vitro*, RT-qPCR was used. As expected, the overexpression of miR-15a-5p significantly downregulated the mRNA expression levels of eotaxin-1, GM-CSF and MUC5AC in IL-13-treated HNECs (Fig. 5A-C). In contrast, the inhibitory effect of miR-15a-5p mimics was significantly reversed following JAK2 overexpression (Fig. 5A-C). Similarly, the anti-inflammatory effect of miR-15a-5p on the secretory levels of these proteins was significantly reversed by JAK2 overexpression (Fig. 5D-F). All these data indicated that the upregulation of JAK2 may rescue the anti-inflammatory effect of miR-15a-5p mimics on AR.

Discussion

Although increasing efforts have been made to improve the treatment of AR, the disease remains difficult to manage and significantly affects the patients' quality of life (38). Hence, it is necessary to discover novel methods for AR treatment. In the present study, HNECs were treated with IL-13 to study AR in vitro. The results revealed that the production of GM-CSF, eotaxin-1 and MUC5AC was significantly increased

following IL-13 treatment, confirming that the *in vitro* model of AR had been successfully established. GM-CSF, eotaxin-1 and MUC5AC are known as key mediators in AR due to the fact that upregulation of these three cytokines is associated with the progression of AR (15,32). Thus, the present findings suggested that ANRIL could mediate the progression of AR via regulation of GM-CSF, eotaxin-1 and MUC5AC.

Previous studies have revealed that lncRNAs participate in AR. For example, lncRNA growth arrest specific 5 was found to inhibit the progression of AR via regulation of immune responses (14). Another previous study indicated that linc00632 suppressed the inflammatory cytokine effects caused by IL-13 and mucin production in neuroepithelial cells (15). In the current study, ANRIL was found to be activated in IL-13-treated HNECs. This discrepancy may result from the different functions of lncRNAs on IL-13-induced inflammatory responses. Qian *et al* (16) reported that ANRIL promoted AR via the regulation of inflammatory cytokines (TNF-α, IL-4, IL-6, IL-13, IL-10 and IL-17). The data of the present study were consistent with this previous finding, verifying that ANRIL knockdown could inhibit the occurrence of AR *in vitro* by downregulating the production of inflammatory cytokines and mucus. Of note, Zhou *et al* (39) discovered that silencing ANRIL could sponge miR-125a-5p to inhibit the progression of Alzheimer's disease. However, the findings of the present study revealed that ANRIL could bind to miR-

15a-5p in AR. Therefore, ANRIL may play a role in different types of diseases by regulating different miRNAs.

miRNAs are common negative regulators of gene expression. According to the competitive endogenous RNA (ceRNA) mechanism, endogenous lncRNAs with miRNA target sites have the potential to act as natural miRNA sponges, which suppress the expression of miRNA targets by competitively binding and inhibiting miRNAs (40). Notably, some lncRNAs (PVT1 and FENDRR) have been identified to regulate miR-15a-5p expression via the ceRNA network (41,42). The current data identified potential crosstalk between ANRIL and miR-15a-5p, suggesting that ANRIL knockdown inhibited the progression of AR by preventing the sponging of miR-15a-5p. Additionally, it has been previously reported that miR-15a-5p could promote the progression of sepsis by regulating the inflammatory response in macrophages and targeting TNFAIP3-interacting protein 2 (43). In the present research, the overexpression of miR-15a-5p could inhibit the development of AR *in vitro* by suppressing the secretion of GM-CSF, eotaxin-1 and MUC5AC. Thus, these findings indicated that miR-15a-5p may serve as a suppressor during inflammation. Wang *et al* (28) reported that miR-15a-5p inhibited IL-13-induced expression of GM-CSF, eotaxin-1 and MUC5AC in HNECs to alleviate AR via negatively regulating adrenoceptor β2 (ADRB2). The findings of the current study were consistent with this previous study, indicating that miR-15a-5p may serve as a suppressor in AR.

In addition, JAK2 was discovered to be directly targeted by miR-15a-5p. JAK2/STAT3 is an important signaling pathway involved in multiple inflammatory responses (44,45). For example, JAK2/STAT3 was reported to promote the inflammatory responses induced by lipopolysaccharide in human umbilical vein endothelial cells (46). Moreover, JAK2/STAT3 has been proven to be a key mediator of Th2-mediated immune responses (47). Paroxetine was identified to exert its immunosuppressive effects on immune responses by activating the JAK2/STAT3 signaling pathway (48), suggesting that the JAK2/STAT3 signaling pathway has immunosuppressive effect, which is the opposite function found in other previous studies. This phenomenon may due to the different type of diseases. In the present study, the overexpression of JAK2 significantly suppressed the anti-inflammatory effects of miR-15a-5p in AR. Wang *et al* (30) reported that miR-375 could ameliorate AR via the downregulation of the JAK2/STAT3 signaling pathway. Accordingly, the present findings suggested that miR-15a-5p may exert its anti-inflammatory effect in IL-13-treated HNECs by targeting JAK2 and inactivating JAK2/STAT3 signaling. However, it should be noted that this study only focused on JAK2/STAT3 signaling. Since IL-4 secreted by Th2 cells has also been reported to be involved in AR (15), the effect of ANRIL on IL-4 production should be further investigated in the future.

In conclusion, the findings of the present study suggested that ANRIL may function as a mediator in AR. ANRIL knockdown was demonstrated to exert its anti-inflammatory effect in IL-13-treated HNECs via regulation of the miR-15a-5p/JAK2/STAT3 axis. These results suggested that ANRIL may serve as a novel target for the treatment of AR.

Acknowledgements

Not applicable.

Availability of data and materials

All data generated or analyzed during this study are included in this published article.

Authors' contributions

H-WL designed the study, performed the experiments, prepared the manuscript and acted as the guarantor of the integrity of the entire study. Y-QZ designed the study, analyzed the data and reviewed the manuscript. Z-LH analyzed the data and reviewed the manuscript. HL, Q-FT and JT performed the experiments. All authors read and approved the final manuscript.

Ethics approval and consent to participate

Not applicable.

Patient consent for publication

Not applicable.

Competing interests

These authors declare that they have no competing interests.

References

1. Greiner AN, Hellings PW, Rotiroti G and Scadding GK: Allergic rhinitis. Lancet 378: 2112-2122, 2011.
2. Li L, Zhang L, Mo JH, Li YY, Xia JY, Bai XB, Xie PF, Liang JY, Yang ZF and Chen QY: Efficacy of indoor air purification in the treatment of Artemisia pollen-allergic rhinitis: A randomised, double-blind, clinical controlled trial. Clin Otolaryngol 45: 394-401, 2020.
3. Pazdro-Zastawny K, Kolator M, Krajewska J, Basiak-Rasała A, Górna S, Paluszkiewicz P, Zatoński M and Zatoński T: Lifestyle-related factors differentiating the prevalence of otorhinolaryngological diseases among 6-17-year-olds from Wrocław, Poland. Int J Pediatr Otorhinolaryngol 132: 109934, 2020.
4. Licari A, Castagnoli R, De Filippo M, Foiadelli T, Tosca MA, Marseglia GL and Ciprandi G: Current and emerging biologic therapies for allergic rhinitis and chronic rhinosinusitis. Expert Opin Biol Ther 20: 609-619, 2020.
5. Liu J, Zhang X, Zhao Y and Wang Y: The association between allergic rhinitis and sleep: A systematic review and meta-analysis of observational studies. PLoS One 15: e0228533, 2020.
6. Liang ZY, Deng YQ and Tao ZZ: A quantum dot-based lateral flow immunoassay for the rapid, quantitative, and sensitive detection of specific IgE for mite allergens in sera from patients with allergic rhinitis. Anal Bioanal Chem 412: 1785-1794, 2020.
7. Kenyon CC, Maltenfort MG, Hubbard RA, Schinasi LH, De Roos AJ, Henrickson SE, Bryant-Stephens TC and Forrest CB: Variability in diagnosed asthma in young children in a large pediatric primary care network. Acad Pediatr 20: 958-966, 2020.
8. Choi HS, Kim SL, Kim JH and Lee DS: The FDA-approved anti-asthma medicine ciclesonide inhibits lung cancer stem cells through Hedgehog signaling-mediated SOX2 regulation. Int J Mol Sci 21: 1014, 2020.
9. Yi L, Cui Y, Xu Q and Jiang Y: Stabilization of LSD1 by deubiquitinating enzyme USP7 promotes glioblastoma cell tumorigenesis and metastasis through suppression of the p53 signaling pathway. Oncol Rep 36: 2935-2945, 2016.

10. Qin X, Zhu S, Chen Y, Chen D, Tu W and Zou H: Long non-coding RNA (lncRNA) CASC15 is upregulated in diabetes-induced chronic renal failure and regulates podocyte apoptosis. Med Sci Monit 26: e919415, 2020.

11. Zhao J, Pu J, Hao B, Huang L, Chen J, Hong W, Zhou Y, Li B and Ran P: LncRNA RP11-86H7.1 promotes airway inflammation induced by TRAPM2.5 by acting as a ceRNA of miRNA-9-5p to regulate NFKB1 in HBECS. Sci Rep 10: 11587, 2020.

12. Liu X, Zhu N, Zhang B and Xu SB: Long Noncoding RNA TCONS_00016406 attenuates lipopolysaccharide-induced acute kidney injury by regulating the miR-687/PTEN pathway. Front Physiol 11: 622, 2020.

13. Yang Y, Zhang Y, Yang Y, Guo J, Yang L, Li C and Song X: Differential expression of long noncoding RNAs and their function-related mRNAs in the peripheral blood of allergic rhinitis patients. Am J Rhinol Allergy 34: 508-518, 2020.

14. Zhu X, Wang X, Wang Y and Zhao Y: Exosomal long non-coding RNA GAS5 suppresses Th1 differentiation and promotes Th2 differentiation via downregulating EZH2 and T-bet in allergic rhinitis. Mol Immunol 118: 30-39, 2020.

15. Yue L, Yin X, Hao F, Dong J, Ren X, Xu O and Shan C: Long noncoding RNA linc00632 inhibits interleukin-13-induced inflammatory cytokine and mucus production in nasal epithelial cells. J Innate Immun 12: 116-128, 2020.

16. Qian X, Shi S and Zhang G: Long non-coding RNA antisense non-coding RNA in the INK4 locus expression correlates with increased disease risk, severity, and inflammation of allergic rhinitis. Medicine (Baltimore) 98: e15247, 2019.

17. Li J, Xu X, Wei C, Liu L and Wang T: Long noncoding RNA NORAD regulates lung cancer cell proliferation, apoptosis, migration, and invasion by the miR-30a-5p/ADAM19 axis. Int J Clin Exp Pathol 13: 1-13, 2020.

18. Yan Y, Peng Y, Ou Y and Jiang Y: MicroRNA-610 is downregulated in glioma cells, and inhibits proliferation and motility by directly targeting MDM2. Mol Med Rep 14: 2657-2664, 2016.

19. Chickooree D, Zhu K, Ram V, Wu HJ, He ZJ and Zhang S: A preliminary microarray assay of the miRNA expression signatures in buccal mucosa of oral submucous fibrosis patients. J Oral Pathol Med 45: 691-697, 2016.

20. Wang H, Guo Y, Mi N and Zhou L: miR-101-3p and miR-199b-5p promote cell apoptosis in oral cancer by targeting BICC1. Mol Cell Probes 52: 101567, 2020.

21. Hawkins LJ and Storey KB: MicroRNA expression in the heart of Xenopus laevis facilitates metabolic adaptation to dehydration. Genomics 112: 3525-3536, 2020.

22. Yang X, Zhu X, Yan Z, Li C, Zhao H, Ma L, Zhang D, Liu J, Liu Z, Du N, et al: miR-489-3p/SIX1 axis regulates melanoma proliferation and glycolytic potential. Mol Ther Oncolytics 16: 30-40, 2019.

23. Chen J, Wang J, Li H, Wang S, Xiang X and Zhang D: p53 activates miR-192-5p to mediate vancomycin induced AKI. Sci Rep 6: 38868, 2016.

24. Shen ED, Liu B, Yu XS, Xiang ZF and Huang HY: The effects of miR-1207-5p expression in peripheral blood on cisplatin-based chemosensitivity of primary gallbladder carcinoma. OncoTargets Ther 9: 3633-3642, 2016.

25. Vakkilainen S, Mäkitie R, Klemetti P, Valta H, Taskinen M, Husebye ES and Mäkitie O: A wide spectrum of autoimmune manifestations and other symptoms suggesting immune dysregulation in patients with cartilage-hair hypoplasia. Front Immunol 9: 2468, 2018.

26. Ma Z, Teng Y, Liu X, Li J, Mo J, Sha M and Li Y: Identification and functional profiling of differentially expressed long non-coding RNAs in nasal mucosa with allergic rhinitis. Tohoku J Exp Med 242: 143-150, 2017.

27. Liu HC, Liao Y and Liu CQ: miR-487b mitigates allergic rhinitis through inhibition of the IL-33/ST2 signaling pathway. Eur Rev Med Pharmacol Sci 22: 8076-8083, 2018.

28. Wang L, Lv Q, Song X, Jiang K and Zhang J: ADRB2 suppresses IL-13-induced allergic rhinitis inflammatory cytokine regulated by miR-15a-5p. Hum Cell 32: 306-315, 2019.

29. Zhu M, Yang M, Yang Q, Liu W, Geng H, Pan L, Wang L, Ge R, Ji L, Cui S, et al: Chronic hypoxia-induced microvessel proliferation and basal membrane degradation in the bone marrow of rats regulated through the IL-6/JAK2/STAT3/MMP-9 pathway. BioMed Res Int 2020: 9204708, 2020.

30. Wang T, Chen D, Wang P, Xu Z and Li Y: miR-375 prevents nasal mucosa cells from apoptosis and ameliorates allergic rhinitis via inhibiting JAK2/STAT3 pathway. Biomed Pharmacother 103: 621-627, 2018.

31. Tang H, Wang H, Bai J, Ding M, Liu W, Xia W, Luo Q, Xu G, Li H and Fang J; Nasal Health Group and China: Sensitivity of MUC5AC to topical corticosteroid is negatively associated with interleukin-17A in patients with allergic rhinitis. Am J Rhinol Allergy 26: 359-364, 2012.

32. Zhai KF, Zheng JR, Tang YM, Li F, Lv YN, Zhang YY, Gao Z, Qi J, Yu BY and Kou JP: The saponin D39 blocks dissociation of non-muscular myosin heavy chain IIA from TNF receptor 2, suppressing tissue factor expression and venous thrombosis. Br J Pharmacol 174: 2818-2831, 2017.

33. Zhai KF, Duan H, Cui CY, Cao YY, Si JL, Yang HJ, Wang YC, Cao WG, Gao GZ and Wei ZJ: Liquiritin from glycyrrhiza uralensis attenuating rheumatoid arthritis via reducing inflammation, suppressing angiogenesis, and inhibiting MAPK signaling pathway. J Agric Food Chem 67: 2856-2864, 2019.

34. Livak KJ and Schmittgen TD: Analysis of relative gene expression data using real-time quantitative PCR and the 2(-ΔΔC(T)) Method. Methods 25: 402-408, 2001.

35. Zhai KF, Duan H, Chen Y, Khan GJ, Cao WG, Gao GZ, Shan LL and Wei ZJ: Apoptosis effects of imperatorin on synoviocytes in rheumatoid arthritis through mitochondrial/caspase-mediated pathways. Food Funct 9: 2070-2079, 2018.

36. Ma Y, Shi L and Zheng C: Microarray analysis of lncRNA and mRNA expression profiles in mice with allergic rhinitis. Int J Pediatr Otorhinolaryngol 104: 58-65, 2018.

37. Teng Y, Zhang R, Liu C, Zhou L, Wang H, Zhuang W, Huang Y and Hong Z: miR-143 inhibits interleukin-13-induced inflammatory cytokine and mucus production in nasal epithelial cells from allergic rhinitis patients by targeting IL13Rα1. Biochem Biophys Res Commun 457: 58-64, 2015.

38. Incorvaia C, Cavaliere C, Frati F and Masieri S: Allergic rhinitis. J Biol Regul Homeost Agents 32 (Suppl 1): 61-66, 2018.

39. Zhou B, Li L, Qiu X, Wu J, Xu L and Shao W: Long non-coding RNA ANRIL knockdown suppresses apoptosis and pro-inflammatory cytokines while enhancing neurite outgrowth via binding microRNA-125a in a cellular model of Alzheimer's disease. Mol Med Rep 22: 1489-1497, 2020.

40. Ping Y, Zhou Y, Hu J, Pang L, Xu C and Xiao Y: Dissecting the functional mechanisms of somatic copy-number alterations based on dysregulated ceRNA networks across cancers. Mol Ther Nucleic Acids 21: 464-479, 2020.

41. Wu H, Tian X and Zhu C: Knockdown of lncRNA PVT1 inhibits prostate cancer progression in vitro and in vivo by the suppression of KIF23 through stimulating miR-15a-5p. Cancer Cell Int 20: 283, 2020.

42. Zhu Y, Zhang X, Wang L, Zhu X, Xia Z, Xu L and Xu J: FENDRR suppresses cervical cancer proliferation and invasion by targeting miR-15a/b-5p and regulating TUBA1A expression. Cancer Cell Int 20: 152, 2020.

43. Lou Y and Huang Z: microRNA-15a-5p participates in sepsis by regulating the inflammatory response of macrophages and targeting TNIP2. Exp Ther Med 19: 3060-3068, 2020.

44. Yu L, Liu Z, He W, Chen H, Lai Z, Duan Y, Cao X, Tao J, Xu C, Zhang Q, et al: Hydroxysafflor yellow A confers neuroprotection from focal cerebral ischemia by modulating the crosstalk between JAK2/STAT3 and SOCS3 signaling pathways. Cell Mol Neurobiol 40: 1271-1281, 2020.

45. Fang XY, Zhang H, Zhao L, Tan S, Ren QC, Wang L and Shen XF: Corrigendum to 'A new xanthatin analogue 1β-hydroxyl-5α-chloro-8-epi-xanthatin induces apoptosis through ROS-mediated ERK/p38 MAPK activation and JAK2/STAT3 inhibition in human hepatocellular carcinoma' [Biochimie 152C (2018) 43-52]. Biochimie 171-172: 21-22, 2020.

46. Wang J, Du A, Wang H and Li Y: MiR-599 regulates LPS-mediated apoptosis and inflammatory responses through the JAK2/STAT3 signaling pathway via targeting ROCK1 in human umbilical vein endothelial cells. Clin Exp Pharmacol Physiol 47: 1420-1428, 2020.

47. Peng DH, Liu YY, Chen W, Hu HN and Luo Y: Epidermal growth factor alleviates cerebral ischemia-induced brain injury by regulating expression of neutrophil gelatinase-associated lipocalin. Biochem Biophys Res Commun 524: 963-969, 2020.

48. Kabiri M, Hemmatpour A, Zare F, Hadinedoushan H and Karimollah A: Paroxetine modulates immune responses by activating a JAK2/STAT3 signaling pathway. J Biochem Mol Toxicol 34: e22464, 2020.